

Transport and confinement in JT-60SA

E. Barbato¹, C. Angioni², L. Garzotti³, G. Giruzzi⁴, X. Litaudon⁴, M. Romanelli³, M. Yoshida⁵, K. Tanaka⁶, N. Hayashi⁵, Y. Kamada⁵, JT-60SA Research Plan Contributors and the JT-60SA Team

¹ Associazione EURATOM ENEA sulla Fusione, CP 65-00044-Frascati, Rome, Italy, ²Max Planck Institut fuer Plasmaphysik, EURATOM Association, Boltzmannstrasse 2 85748 Garching, Germany, ³EURATOM/CCFE Fusion Association, Culham Science Centre, Abingdon, Oxon OX14 3DB, United Kingdom, ⁴CEA, IRFM, F-13108 St Paul Lez Durance, France, ⁵Japan Atomic Energy Agency, Naka, Ibaraki-ken, 311-0193, Japan, ⁶National Institute for Fusion Science, 322-6 Oroshi-cho, Toki 509-5292, Japan

1. Introduction. In this paper we focus on plasma transport and confinement experiments and studies envisaged on JT-60SA [1]. JT-60SA can operate highly shaped, long lasting discharges while heating both ions and electrons through flexible NBI and ECRF systems. Transport and confinement studies will take advantage from these features and will focus on those experimental regimes, useful for ITER and DEMO, which can be attained in high beta Advanced Tokamak regimes [2]. In section 2 the main confinement issues and transport regimes, highlighting the specific contribution of JT-60SA to the fusion program, are discussed. Section 3 shows how JT-60SA, by virtue of its auxiliary heating systems, can cover a wide region of the dimensionless plasma parameters space and can access the ITER- and DEMO-relevant values of v^* , ρ^* . In section 4 a first fully predictive (100s) 1.5 D transport simulation of an inductive scenario (H-mode) with pellets fuelling is presented and discussed. The transport and confinement results presented here, along with other results [3-5] also presented at this conference, are part of studies [1] that cover many areas relevant to JT-60SA.

2. Main objectives and confinement issues. JT-60SA is designed to operate in Advanced Tokamak regimes: therefore one of the main objective is to study the mutual interaction amongst plasma pressure, rotation and current profiles in high β , highly self-regulating, plasmas: Fig. 1.a shows the area covered by JT-60SA in the bootstrap current fraction, normalized beta (F_{BS} , β_N) plane, thus tracing the way from JET and JT-60U to ITER and DEMO (the points in the figures result from several cross-checked 0-D transport calculations [1, 6] and they are representative of the SA scenarios reported in the Table 2-3 of ref. [1]). Fig 1.b shows the envisaged high confinement regimes at high-density, above the Greenwald density. This is another important feature of these advanced scenarios and will be achieved through the control of the plasma profiles, plasma shape and particle fueling. Studies of the energy and particle confinement scaling, both on hybrid and high β scenarios, at high plasma shaping, will also be possible due to the high JT-60SA shaping capability. The heating

system (24 MW of Positive NBI, 10MW of Negative NBI and 7 MW of ECRH) allows to vary the electron heating power to the total input power from $\sim 20\%$ to $\sim 70\%$ with low external fuelling and torque input (by NNBI and ECRH only, at $P_{\text{TOT}} > 20\text{MW}$, that is larger than the power threshold for the L-H transition). Therefore heat, particle and momentum transport properties can be studied in dominant electron heating conditions. Furthermore, by varying both the ratio of electron heating power and the electron density, transport studies can be led at different T_i/T_e ratio, thus contributing to investigate the role of the heating ratio, T_i/T_e collisionality and electron β on density peaking [7] and toroidal rotation. Figs. 2a and 2b show the T_i/T_e ranges calculated by METIS [6], as they result from density scan at fixed power (2a) and ECRH power scan (2b) at fixed density. Finally the presence of a large population of fast ions due to NBI allows also studying stabilization of the ITG turbulence through optimization of the normalized pressure gradient α [8].

3. Dimensionless parameter space. By virtue of its auxiliary heating systems JT-60SA allows transport experiments covering a wide region of the dimensionless plasma parameters space and will access (although not simultaneously and at a value of the aspect ratio smaller than in ITER) the ITER [9] and DEMO [2] relevant values of the normalized collisionality (ν^*), poloidal Larmor radius (ρ_p^*) and beta (β_N) with ITER and DEMO-like plasma shapes (Figs. 3a and 3b). (In Fig. 3b the accessible values in the (β_N, ρ_p^*) plane are shown at fixed ν^* , assuming $H_{\text{ITER89Y2}}=1$). The non-dimensional plasma parameters mentioned above have a direct impact on small-scale fluctuations and hence on turbulent transport. The transport of particle, impurity, heat, and momentum in advanced tokamaks is dominated by turbulence-driven anomalous transport. Decay time of zonal flow relates to ion-ion collision frequency and the radial scale of zonal flow relates to ion Larmor radius. Thus, it is crucial to understand and clarify the driving and stabilizing mechanisms of turbulence also in the absence of transient collisional effects and in ITER- and DEMO-relevant regimes (low ν^* and ρ_p^*). The knowledge of turbulence driven transport is required to design steady state operation scenarios in both ITER and DEMO. Several core turbulence modes are expected. Each turbulence mechanism plays a role on different aspects of the transport process. Detailed turbulence measurements by using proper diagnostic will be investigated with focus on both the core and the pedestal and a comparison with theoretical predictions will be carried out. A specific contribution of JT-60SA to ITER H-mode operations will concern the parameter dependences of H-mode threshold power in H and He plasmas well in advance of ITER operations. Transport physics and scaling of the pedestal will be studied in support for the

prediction of the H-mode threshold power for ITER and to allow designing operation scenarios in ITER able to achieve the H-mode phase efficiently. Experiments in JT-60SA will provide a new insight of transport physics, which does not appear in the short pulse experiments. Probabilistic approach will be introduced through the plasma parameter (e.g. β_N) dependence for understanding of sustainment of high beta plasmas. Finally in future burning plasma experiments, the external momentum input from the auxiliary heating is expected to be small and the associated toroidal rotation velocity may not dominate the intrinsic plasma rotation. It is therefore essential to understand the physical mechanisms determining the toroidal rotation profile including the intrinsic rotation. Study on the intrinsic rotation will be made at high pressure and in a small or no torque input using a combination of NBI and ECRF, at lower ρ^* with respect to present devices.

4. First fully predictive (100s) transport simulations of inductive H-mode scenario. The JINTRAC suite of codes and the ASTRA code were used for this study. The plasma parameters are those of scenario 2 (table 2-3 ref. [1]). Semi-empirical Bohm-gyroBohm transport models [10, 11], mainly tuned on JET data [12], were assumed in both codes. In JINTRAC, the continuous ELM model [12] is assumed to describe transport into the pedestal region (i.e. transport is adjusted to keep the normalized pressure gradient α less than a prescribed critical value, α_c , for the ballooning instability). Increasing the prescribed value of α_c makes the pressure on the top of the pedestal higher. To control the plasma density, pellets are injected from the LFS at a velocity of 300 m/s. A feedback mechanism on the pellet injection controls the volume-average density $\langle n_e \rangle$. The pellet deposition profile is calculated by the NGPS code [13] (see Fig.4b) and the pellet injection frequency is one of the results of the whole calculation. Three cases have been considered with different limiting α_c values (1.3, 1.5, 1.7). The electron temperature and plasma density profiles are shown in Figs. 4a and 4b for the three values of α_c . Changing α_c does not affect the density (due to the feedback on pellets injection) while it affects the temperature at the top of the pedestal. The main results of these calculations are: i) an H factor (with respect to ITER98Y2 [6] scaling) in the range 1.1 and 1.3 is obtained when increasing α_c ; ii) a pellet injection frequency between 15 and 17 Hz is needed to control the plasma density. The results obtained by ASTRA simulations are shown in Fig. 4c. Here an H factor of 1.1 is obtained as well as a bootstrap current fraction of 22%. In the ASTRA simulations the temperature at the top of the pedestal region is assumed as a boundary condition for the core transport calculation. This value is somewhat lower than predicted by the JINTRAC simulations at high α_c .

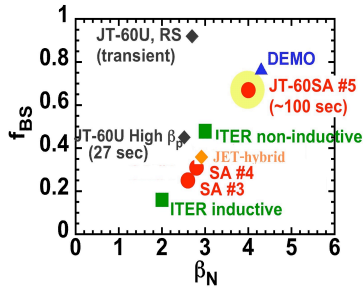


Fig.1a: The bootstrap current fraction (f_{BS}) against the normalized beta (β_N)

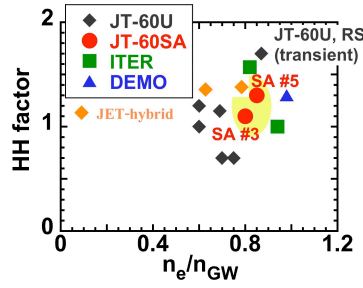


Fig.1b: Target regimes in the plane HH factor - Greenwald Density fraction (n_e/n_{GW}).

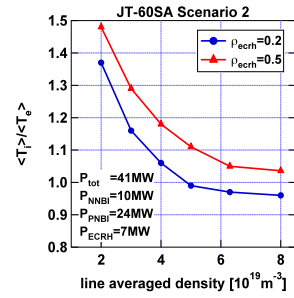


Fig.2a: T_i/T_e ratio vs. density at fixed ECRH power. The two curves refer to different ECRH deposition radii.

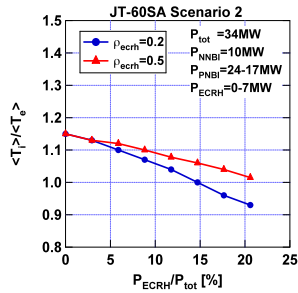


Fig.2b: T_i/T_e ratio vs. ECRH power at fixed density

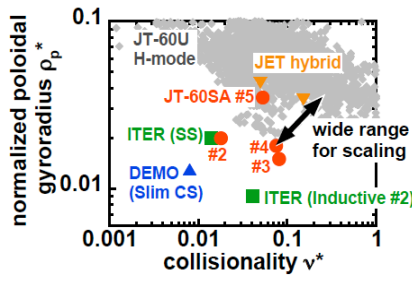


Fig.3a: Non-dimensional plasma parameter regimes of JT-60SA.

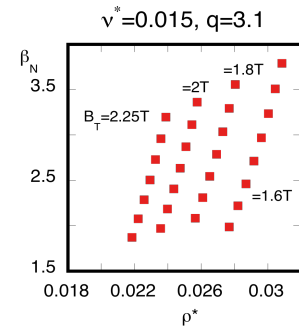


Fig.3b: Accessible values of β_N vs ρ^* at fixed ν^* ($H=1$).

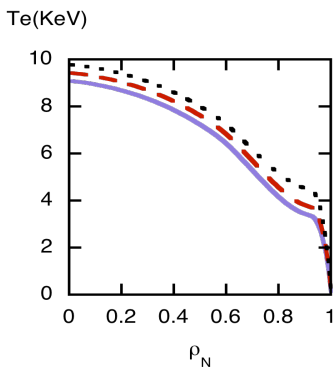


Fig.4a: T_e profiles from JINTRAC simulations of scenario 2 at $\alpha_c = 1.3, 1.5, 1.7$.

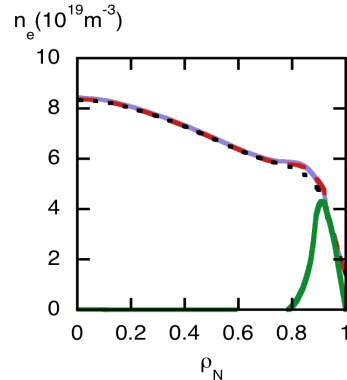


Fig.4b: Density profiles at different α_c and pellet deposition profile from NGPS-JINTRAC (right).

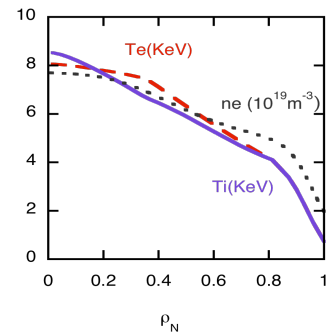


Fig.4c: T_e, T_i from ASTRA simulations of scenario 2. The n_e profile (dotted line) is assumed.

References

[1] JT-60SA Research Plan V3 (2011), http://www.jt60sa.org/pdfs/JT-60SA_Res_Plan.pdf
 [2] K. Tobita et al., Nucl. Fusion 49 (2009), 075029
 [3] G. Giruzzi et al. 2012 39th EPS Conf. on Controlled Fusion and Plasma Physics P5.018
 [4] T. Bolzonella et al 2012 39th EPS Con. on Controlled Fusion and Plasma Physics f P4.025
 [5] J. Garcia et al 2012 39th EPS Conf. on Controlled Fusion and Plasma Physics P5.057
 [6] J.F. Artaud et al. 2005 in 32nd EPS Conf. on Controlled Fusion and Plasma Physics, ECA Vol. 29C, P1.035
 [7] C. Angioni et al 2009 Plasma Phys and Contr. Fus 51 12417
 [8] M Romanelli et al 2010 Plasma Phys. Control. Fusion 52 045007 [doi:10.1088/0741-3335/52/4/045007](https://doi.org/10.1088/0741-3335/52/4/045007).
 [9] ITER Phys. E.G 1999 Nucl. Fusion 39 2175
 [10] Vlad et al 1998 Nucl. Fusion 3 557
 [11] Hannum et al 2001 Phys. of Plasmas 8 964
 [12] L. Garzotti et al 2012 Nucl. Fusion 52 013002 [doi:10.1088/0029-5515/52/1/013002](https://doi.org/10.1088/0029-5515/52/1/013002)
 [13] L. Garzotti et al 1997 Nucl. Fusion 37 1167